Shape Evolution and Size-Controllable Synthesis of Cu 2 O Octahedra and Their Morphology-Dependent Photocatalytic Properties

ARTICLE *in* THE JOURNAL OF PHYSICAL CHEMISTRY B · AUGUST 2006

Impact Factor: 3.3 · DOI: 10.1021/jp061934y · Source: PubMed

3 AUTHORS, INCLUDING:

Haolan Xu
University of South Australia
48 PUBLICATIONS **2,548** CITATIONS
SEE PROFILE

Wenzhong Wang
Minzu University of China
212 PUBLICATIONS **7,695** CITATIONS
SEE PROFILE

Shape Evolution and Size-Controllable Synthesis of Cu_2O Octahedra and Their Morphology-Dependent Photocatalytic Properties

Haolan Xu, Wenzhong Wang,* and Wei Zhu

State Key Laboratory of High Performance Ceramics and Superfine Microstructure, Shanghai Institute of Ceramics, Chinese Academy of Sciences, 1295 DingXi Road, Shanghai 200050, P. R. China

Received: March 29, 2006; In Final Form: May 30, 2006

Octahedral Cu_2O crystals with tunable edge length were synthesized by reducing copper hydroxide with hydrazine without using any surfactant. Systematic experiments were carried out to investigate the factors which impact on the morphology and size of the products. The molar ratios of the reagents (NH_3:Cu^{2+} and OH^-:Cu^{2+}) determined the morphology and size of the corresponding products via affecting the coordination between NH_3 and Cu^{2+}. It is demonstrated that the ratio of growth rate along ⟨111⟩ versus ⟨100⟩ was varied by adjusting the molar ratio of NH_3 to Cu^{2+}, thus Cu_2O crystals with different morphologies such as spheres, cubelike, and octahedra were obtained. The edge lengths of octahedra can be easily tuned from 130 to 600 nm by adjusting the molar ratio of OH^- to Cu^{2+}. It is an effective and facile method for the controlled synthesis of octahedral Cu_2O. The obtained octahedral Cu_2O particles show improved ability on adsorption and photodegradation of methyl orange compared with cubic Cu_2O particles.

Introduction

In recent years, developing ways of tailing the structure of materials on specific morphologies has been one of the important goals of material scientists.[1−6] The shape and size of inorganic materials are well-known to have great effects on their widely varying properties.[7,8] Much effort has been devoted to synthesize semiconductor nanoparticles with different morphologies, such as wires, rods,[9] cubes,[10,11] hollow spheres,[12,13] and tetrapods,[14,15] for their specific properties and corresponding potential applications.

As an important p-type semiconductor with a direct band gap of about 2.2 eV, cuprous oxide (Cu_2O) with unique optical and magnetic properties is a promising material with applications in solar energy conversion,[16] as an electrode for lithium ion batteries,[17] and in photocatalytic degradation of organic pollutants and decomposition of water into O_2 and H_2 under visible light.[18,19] In the past decade, much effort has been devoted to shape-controlled synthesis of Cu_2O micro- and nanocrystals, such as liquid-phase synthesis of Cu_2O nanowires,[20] nanocubes,[21,22] and hollow spheres,[23,24] and electrodeposition methods for Cu_2O nanocubes.[25] In these methods, surfactants such as PEG and CTAB were generally required to control the morphologies and structures of the products. Recently, Shen and co-workers synthesized octahedral Cu_2O via γ-irradiation in Triton X-100 water-in-oil microemulsions. The average edge length of the octahedron-shaped Cu_2O varies as a function of the dose rate.[26] Though Cu_2O crystals with various morphologies have been successfully synthesized, the reports about the preparation of octahedral Cu_2O and the corresponding properties are limited.[26,27] Developing effective and facile methods for the controlled synthesis of octahedral Cu_2O as well as investigating the corresponding growth mechanism are still necessary. Herein we report a facile route for the controlled synthesis of Cu_2O octahedra, in which copper chloride, ammonia solution, sodium hydroxide, and the reducing agent hydrazine were involved. The synthesis does not require the assistance of organic compounds or surfactants. The morphology and size of Cu_2O can be easily controlled by adjusting the concentration of ammonia solution and NaOH solution. The formation mechanism of octahedral Cu_2O was investigated and proposed based on the electron microscopy analysis. The adsorption ability and photocatalytic activity related to their octahedral morphology were also studied with the comparison of cubelike Cu_2O.

Experimental Section

All reagents purchased from the Shanghai Chemical Company were of analytical grade, and were used without further purification. In a typical preparation, $CuCl_2 \cdot 2H_2O$ (0.852 g) was dissolved in deionized water (100 mL). Then NH_3 solution (2.5 mL, 14 M) was added to the $CuCl_2$ solution under constant stirring. A blue precipitate of $Cu(OH)_2$ was produced when NaOH (10 mL, 1 M) was added dropwise to the above solution. After being stirred for 10 min, $N_2H_4 \cdot H_2O$ (1 mL, 85%) was added dropwise into the blue $Cu(OH)_2$ precipitate suspension, with constant stirring for another 10 min. The $Cu(OH)_2$ precipitate gradually turned yellow then red. Then the red precipitate was filtered, washed with deionized water and ethanol several times, and dried at 60 °C for 4 h in a vacuum oven. The as-prepared product was labeled as sample 1.

The powder X-ray diffraction (XRD) analysis was performed with a Rigaku Rotaflex diffractometer. Transmission electron microscopy (TEM) images were recorded by a JEOL JEM-2100F field-emission transmission electron microscope, using an accelerating voltage of 200 kV. Field-emission scanning electron microscopy (FESEM) analysis was conducted with a JEOL JSM-6700F electron microscope.

The adsorption and photodegradation of methyl orange under visible light irradiation was selected to study the morphology related properties of these octahedral Cu_2O particles. A 0.1 g sample of octahedral Cu_2O particles with different sizes was

* Address correspondence to this author. Phone: +86-21-5241-5295. E-mail: wzwang@mail.sic.ac.cn.

10.1021/jp061934y CCC: $33.50
Published on Web 06/28/2006

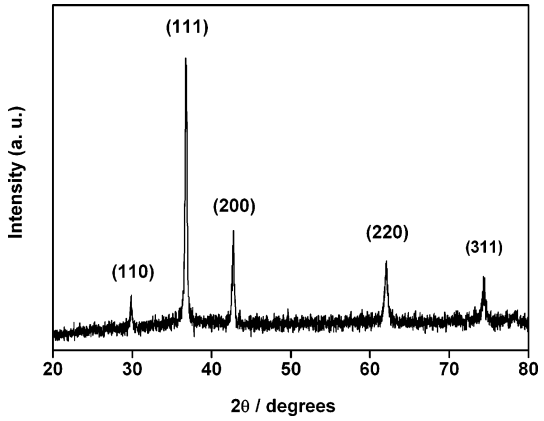

Figure 1. XRD pattern of the octahedral Cu_2O particles.

dispersed in a 100 mL solution of methyl orange (100 mg/L) and mixture was put in a quartz reactor. Before illumination, the suspensions were magnetically stirred in the dark for over 5 h to ensure adsorption equilibrium of methyl orange on the surface of Cu_2O octahedra. The photocatalytic reactions were carried out at room temperature, using a 500-W Hg lamp (Oriel) with a UV cutoff filter ($\lambda > 400$ nm). Methyl orange concentration was analyzed through a UV−vis spectrophotometer (UV-2003). The adsorption ability and the photocatalytic activity of cubelike Cu_2O particles with the same quality (0.1 g) were also investigated as a reference for comparison to study the morphology dependent photocatalytic properties.

Results and Discussion

Figure 1 is the XRD pattern of sample 1 prepared when the molar ratio of Cu^{2+}, NH_3 to OH^- is 1:7:2. All five diffraction peaks are indexed to cubic Cu_2O [JCPDS 34-1354]. No other diffraction peaks arising from possible impurities such as Cu and $Cu(OH)_2$ are detected, indicating pure Cu_2O was obtained under this experimental condition.

The morphology of sample 1 was recorded by FESEM and TEM with different magnifications as shown in Figure 2. Figure 2a shows a panoramic view of the as-prepared product, from which regular octahedral Cu_2O particles with narrow size distribution are demonstrated. The average edge length of these octahedra is measured to be about 130−150 nm (Figure 2b). A corresponding TEM image of an octahedron is shown in Figure 2c. The contrast between the top part and the center part further reveals the octahedral structure. The cubic symmetry of these octahedra is the characteristic of the cubic Cu_2O crystal, which is bounded by eight {111} planes.[27] It is believed that the reduction in surface energy is the primary driving force for simple particle growth, the further reduction in surface energy due to the minimization of high surface energy faces will drive the morphology evolution. Anisotropic crystal growth rates lead to nonspherical structures, which are usually realized when the free surface energies of the various crystallographic planes are significantly different. However, recent studies showed that the selective adsorption of molecules and ions in solution on different crystal faces will also make the nanoparticles grow into various shapes by controlling the growth rates along different crystal directions.[28] In our experiments, the octahedral Cu_2O bound by {111} surfaces were formed owing to the different growth rates along ⟨100⟩ versus ⟨111⟩ directions. Scheme 1a outlines the growth of a Cu_2O octahedron. The ammonia solution with a certain concentration may favor the preferential crystal growth along the ⟨100⟩ direction and make

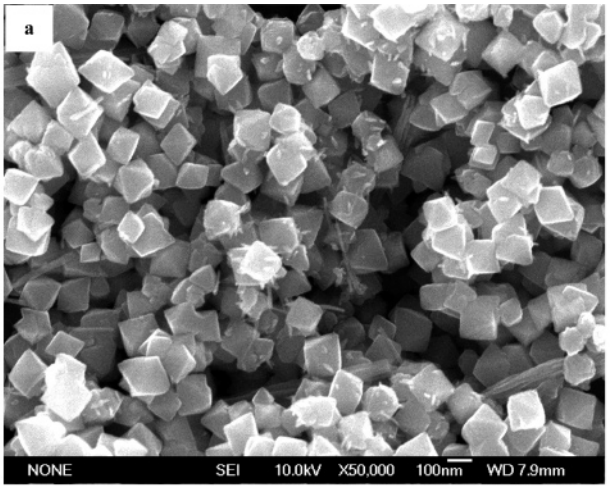

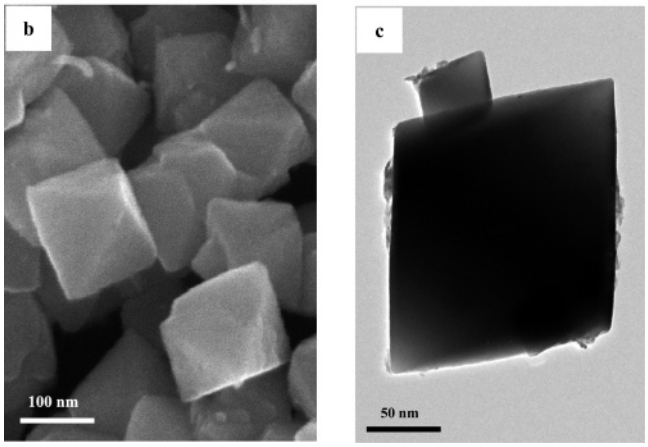

Figure 2. SEM and TEM images of sample 1 (molar ratio of Cu^{2+}, NH_3 to OH^- is 1:7:2): (a, b) SEM image of the Cu_2O octahedra and (c) TEM image of a single octahedron.

SCHEME 1: Schematic Illustration of the Growth Mode of Cu_2O (a) Octahedra and (b) Cubes

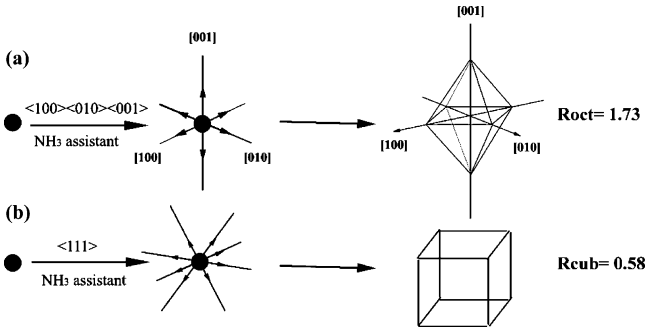

it far exceed that of ⟨111⟩, thus {100} faces shrink. Considering that the growth will be perpendicular to a particular series faces, crystal morphology will be defined by the slowest growing faces ({111} faces in the current case) because the fastest growing faces shrink. Then the octahedra form. It is reported that a perfect octahedron formed when the ratio (R_{oct}) of growth rate along the ⟨100⟩ versus ⟨111⟩ direction is 1.73.[29]

It is found that the molar ratio of NH_3 to Cu^{2+} (defined as R_1) in the system plays an important role in controlling the morphology of the product. Ammonia may influence the morphology of Cu_2O via its coordination property with Cu^{2+}, which will change the growth rates of different crystal directions. When there is no ammonia present in the synthetic system, the

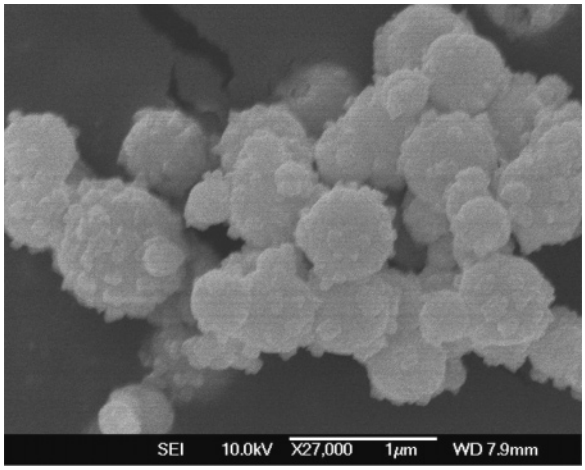

Figure 3. TEM image of the product prepared in the absence of NH_3.

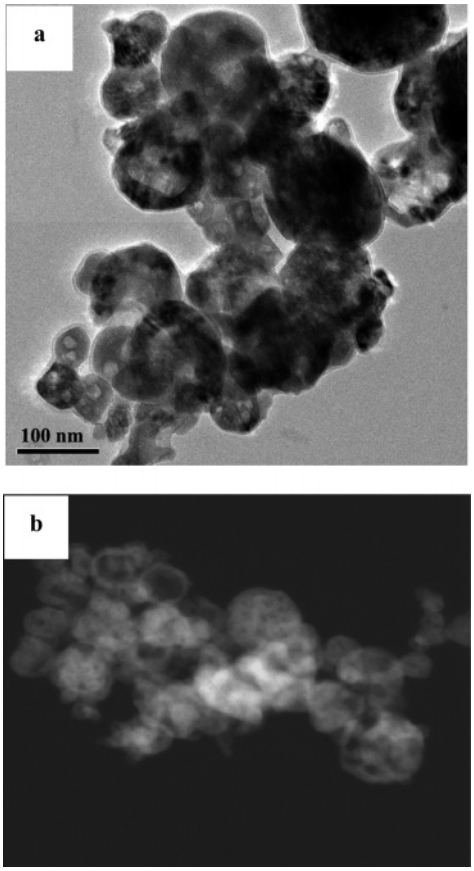

Figure 4. Cu_2O prepared when $R_1 = 1$: (a) TEM image of porous Cu_2O spheres and (b) dark field TEM image of the porous spheres.

resultant product Cu_2O (labeled as sample 2) is spherical as revealed by the SEM image (Figure 3). This implies that the growth rates of various directions are almost the same when ammonia is absent.

Another series of experiments with various R_1 (1:1 and 4:1) values were carried out to investigate the relationship between the concentrations of ammonia solution and the corresponding morphologies of the products, which were labeled as sample 3 ($R_1 = 1$) and sample 4 ($R_1 = 4$), respectively. Figure 4a is the TEM image of sample 3, from which the porous structured Cu_2O spheres are observed. The sizes of the pores in theses spheres are varied from 10 nm to about 20 nm. This special porous structure is further confirmed by a dark-field TEM image of

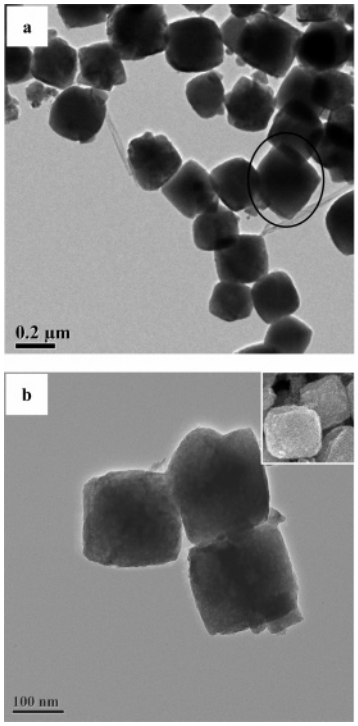

Figure 5. TEM images of cubelike Cu_2O prepared when $R_1 = 4$; the up inset is the SEM image of the cubelike Cu_2O.

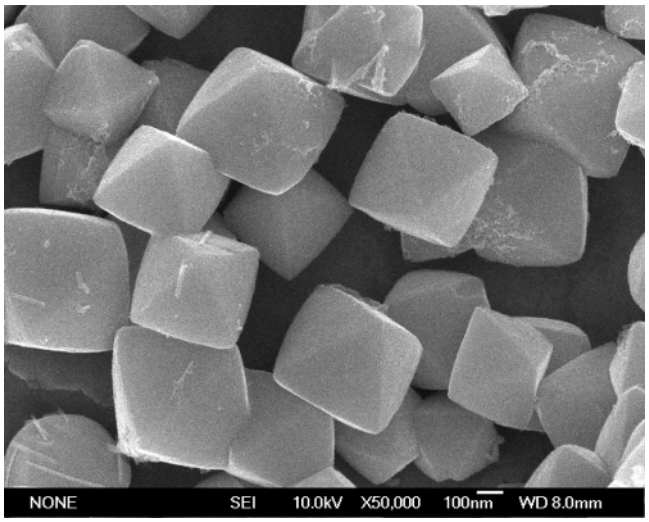

Figure 6. SEM image of octahedral Cu_2O prepared when $R_2 = 4$.

as-prepared Cu_2O (Figure 4b). Hollow spheres are also observed in Figure 4b. The TEM analysis of sample 3 suggests that though the structure of Cu_2O changed (compared with spherical sample 2), the morphology of the products is still spherical. This indicates that when ammonia solution concentration is low, the effect of ammonia on the ratio of growth rate along ⟨111⟩ versus ⟨100⟩ directions is relatively weak.

When the molar ratio of NH_3 to Cu^{2+} (R_1) is 4, cubelike Cu_2O particles (labeled as sample 4, shown in Figure 5) are produced, which is different from the octahedral morphology ($R_1 = 7$) shown in Figure 2c. The average edge length of these Cu_2O cubes is about 180 nm (Figure 5b). As discussed above, the cubic particles bounded by the {100} planes form when the growth rate along the ⟨111⟩ direction far exceeds that of the ⟨100⟩ direction (Scheme 1b). The ratio (named as R_{cub}) of growth rate along the ⟨100⟩ versus the ⟨111⟩ direction is 0.58,

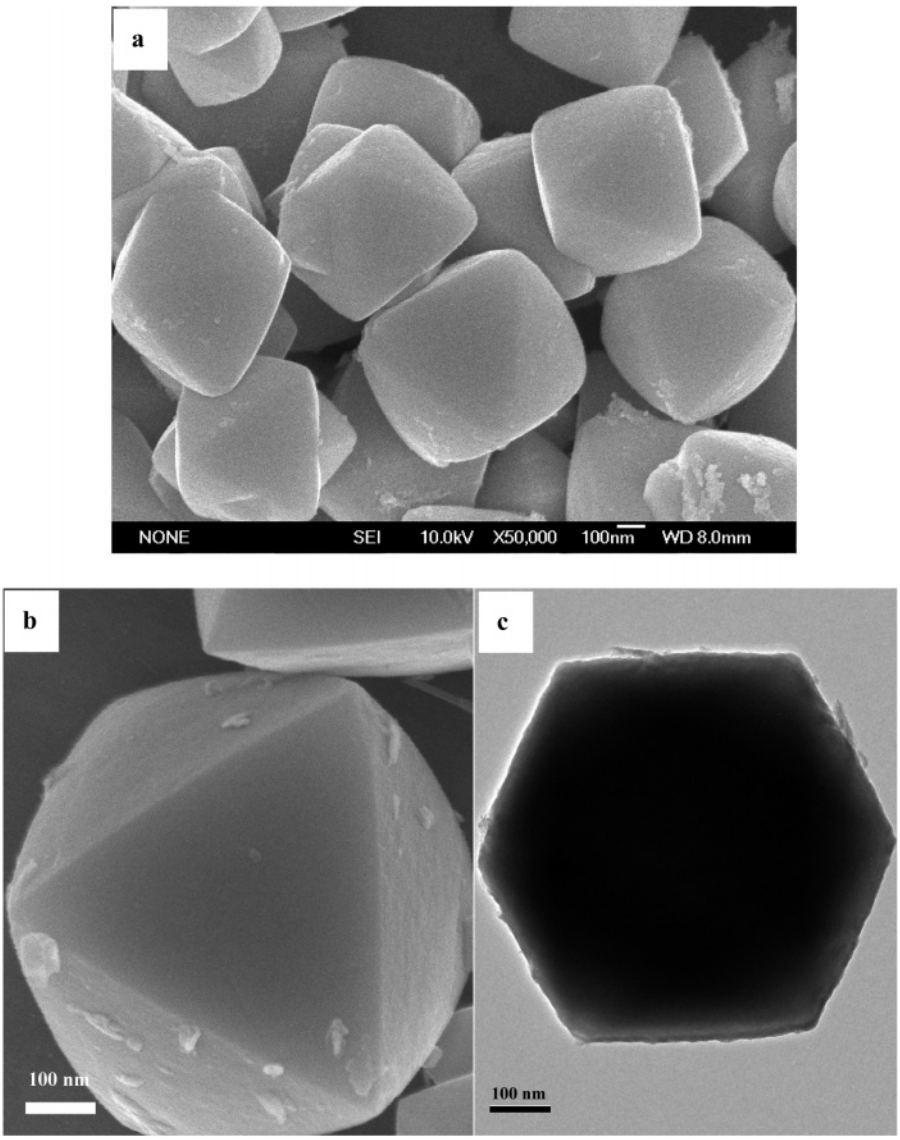

Figure 7. SEM images of octahedral Cu_2O prepared when $R_2 = 8$: (a) the octahedra with longer edge length and (b) an octahedron with arched {111} surfaces and (c) its corresponding TEM image.

which is much lower than that of R_{oct} (1.73).[29] In addition, a small quantity of octahedral particles are also observed (circled in Figure 5a). The coexistence of cubic and octahedral Cu_2O implies that in this stage ($R_1 = 4$) the ratio of growth rate along the ⟨111⟩ versus the ⟨100⟩ direction begins to transform from cubic tendency (R_{cub}) to octahedral tendency (R_{oct}). According to this tendency, we can speculate that when the concentration of NH_3 is increased (R_1 is increased), the cubelike particles will diminish and the octahedron will be the dominant shape. This speculation was well established by sample 1 with uniform octahedral morphology (Figure 2a), which was prepared when R_1 was increased to 7.

The above experiments were carried out to investigate the effect of ammonia solution on the growth rates of different crystallographic directions and the corresponding morphologies of the products. But why ammonia favors preferential growth along the ⟨100⟩ or ⟨111⟩ directions is to be further studied. On the other hand, it is well-established that the pH value plays an important role in wet chemical processing. In the above experiments, the molar ratio of OH^- to Cu^{2+} (defined as R_2) was fixed at 2:1. In this case, partial NH_3 in the $[Cu(NH_3)_4]^{2+}$ complex are replaced by OH^- to form $Cu(OH)_2$ precipitate. When R_2 is higher than 4:1, $[Cu(OH)_4]^{2-}$ will form via replacing more NH_3 in the $[Cu(NH_3)_4]^{2+}$ complex by OH^-.[30] The enhancive replacement of NH_3 by OH^- will weaken the coordination between NH_3 and Cu^{2+}, which will further influence the morphology and the size of the obtained products.

To substantiate our speculation, another series of experiments were carried out via varying R_2 when the molar ratio of NH_3 to Cu^{2+} (R_1) was kept constant (7:1). Figure 6 are the FESEM images of sample 5 that was prepared when R_2 was 4. The morphology of the product is regular octahedral shaped particles. The average edge length size of these octahedra is about 360−420 nm, which is larger than that of sample 1 (Figure 2). When R_2 is increased to 8, much larger Cu_2O octahedra (sample 6) are produced as expected, with an edge length of the octahedra of about 600 nm (Figure 7a). In addition, by comparing sample 5 or sample 6 with sample 1, an interesting phenomenon is observed. The {111} faces of these octahedra are arched surfaces (Figure 7b) in contrast with the planar {111} surfaces of sample 1 (Figure 2b). The corresponding TEM image of octahedral sample 6 is shown in Figure 7c, which was easily misunderstood to be a hexagonal shape or cubic shape in the previous reports. Through the comparison of samples 5, 6, and 1, it is concluded

TABLE 1: Summary of the Experimental Conditions and Corresponding Morphology of Cu_2O

sample	R_1 (NH_3:Cu^{2+})	R_2 (OH^-:Cu^{2+})	shape	size, nm
2	0	2	spheres	400−600
3	1	2	hollow and porous spheres	50−120
4	4	2	cubelike particles	180
1	7	2	octahedral particles	130−150
5	7	4	octahedral particles	360−420
6	7	8	octahedral particles	600

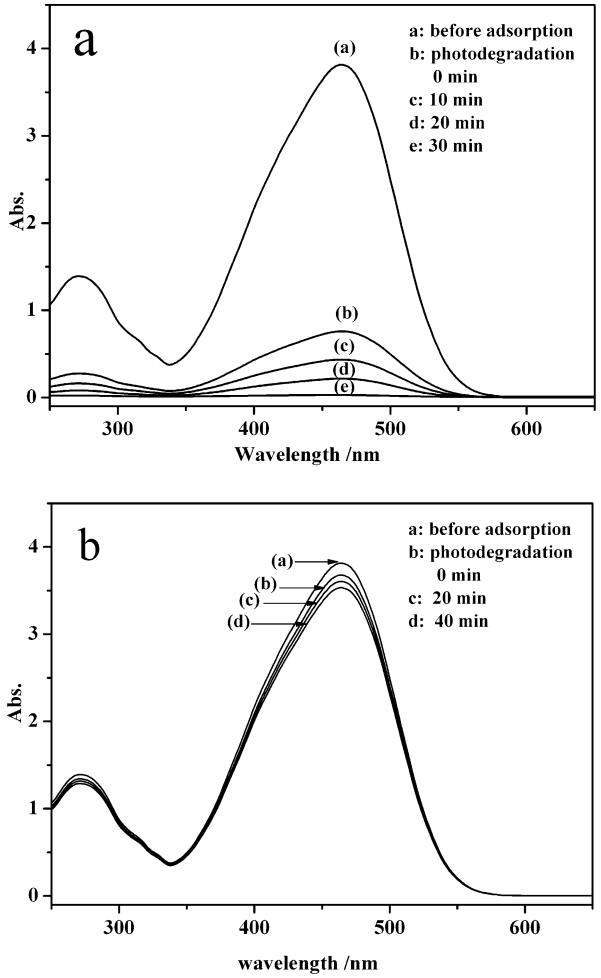

Figure 8. (a) Absorption spectrum of a solution of methyl orange in the presence of Cu_2O octahedra. (b) Absorption spectrum of a solution of methyl orange in the presence of cubic Cu_2O particles.

that the edge lengths of octahedra are increased with the increase of concentration of OH^- (increase of R_2). The size and shape evolution of Cu_2O and their corresponding experimental conditions are summarized in Table 1.

Cu_2O has been used as a photocatalyst for the hydrogen production and organic pollutants degradation under visible light. Previous studies on the photocatalytic activity of Cu_2O were carried out without taking account of its morphology. To demonstrate the potential applicability of the present Cu_2O octahedra (sample 6, 600 nm) related to the morphology, the adsorption ability and photocatalytic activity of Cu_2O octahedra and cubes, which was prepared according to the literature,[21] were compared to study the morphology-dependent photocatalytic property. The degradation of methyl orange was selected as reference and the characteristic absorption of methyl orange at about 465 nm was selected for monitoring the adsorption and photocatalytic degradation process. Figure 8 shows the absorption spectra of an aqueous solution of methyl orange photodegraded by octahedral Cu_2O particles (Figure 8a) and cubic Cu_2O particles (Figure 8b) at different stages, from which one can see that the adsorption ability and the photocatalytic activity of the octahedral Cu_2O particles is much higher than those of the cubic Cu_2O particles. Octahedral Cu_2O adsorb about 80% of the methyl orange in the solution and the degradation rate of methyl orange is about 6 mg min^{-1} g^{-1}, when cubic Cu_2O particles show ignorable either adsorption or degradation of the methyl orange. The adsorption and photocatalytic activity of octahedral Cu_2O particles of sample 1 (130−150 nm) and sample 5 (360−420 nm) were also investigated, which showed better results than that of sample 6. The improvement in photocatalytic activity of octahedral Cu_2O may be ascribed to the exposed {111} surfaces. This finding further implies that adsorptive and photocatalytic activity is related to its morphology and crystal surfaces.

Conclusion

In summary, cuprous oxide octahedra with different edge length were synthesized by utilizing hydrazine as a reductant. The preparation of octahedral Cu_2O does not require the assistance of organic compounds or surfactants, and thus can be considered as a useful inorganic synthesis route. With the assistance of TEM and SEM analysis, the factors which influence the morphology and size of the products were investigated. The concentration of NH_3 solution affects the ratio of the growth rate along the ⟨111⟩ versus the ⟨100⟩ direction, which further conducts the morphology of the product. Cu_2O with different morphologies such as spherical particles, porous spherical particles, cubes, and octahedra were obtained via adjusting the molar ratio of NH_3 to Cu^{2+}. The concentration of NaOH solution altered the edge lengths of the octahedra via influencing the coordination between NH_3 and Cu^{2+}. The edge lengths of octahedra can be easily tuned from 130 to 600 nm via adjusting the molar ratio of OH^- to Cu^{2+}. The adsorption ability and photocatalytic activity of these octahedral Cu_2O particles were investigated with the comparison of cubic Cu_2O particles. The results demonstrate that Cu_2O octahedra with exposed {111} crystal surfaces possess much higher activity than cubes. This investigation may provide a guidance for the shape-controlled synthesis of Cu_2O crystals with tunable size and their application in the treatment of organic pollutants.

Acknowledgment. Financial support form Chinese Academy of Sciences and Shanghai Institute of Ceramics under the program for Recruiting Outstanding Overseas Chinese (Hundred Talents Program) is gratefully acknowledged.

References and Notes

(1) Xie, Y.; Huang, J. X.; Li, B.; Liu, Y.; Qian, Y. T. *Adv. Mater.* **2000**, *12*, 1523−1526.

(2) Sampanthar, J. T.; Zeng, H. C. *J. Am. Chem. Soc.* **2002**, *124*, 6668−6675.

(3) Braun, P. V.; Osenar, P.; Stupp, S. I. *Nature* **1996**, *380*, 325−328.

(4) Lou, X. W.; Zeng, H. C. *J. Am. Chem. Soc.* **2003**, *125*, 2697−2704.

(5) Iijima, S. *Nature* **1991**, *354*, 56−58.

(6) Ohara, P. C.; Heath, J. R.; Gelbart, W. M. *Angew. Chem., Int. Ed. Engl.* **1997**, *36*, 1078−1080.

(7) Alivisatos, A. P. *Science* **1996**, *271*, 933−937.

(8) El-Sayed, M. A. *Acc. Chem. Res.* **2001**, *34*, 257−264.

(9) Xia, Y. N.; Yang, P. D.; Sun, Y. G.; Wu, Y. Y.; Gates, M. B.; Yin. Y. D.; Kim, F.; Yan, H. Q. *Adv. Mater.* **2003**, *15*, 353−389.

(10) Jin, R. C.; Egusa, S.; Scherer, N. F. *J. Am. Chem. Soc*. **2004**, *126*, 9900−9901.
(11) Dumestre, F.; Chaudret, B.; Amiens, C.; Renaud, P.; Fejes, P. *Science* **2004**, *303*, 821−823.
(12) Caruso, F.; Caruso, R. A.; Mohwald, H. *Science* **1998**, *282*, 1111−1114.
(13) Kim, S. W.; Kim, M.; Lee, W. Y.; Hyeon, T. *J. Am. Chem. Soc*. **2002**, *124*, 7642−7643.
(14) Manna, L.; Scher, E. C.; Alivisatos, A. P. *J. Am. Chem. Soc*. **2000**, *122*, 12700−12706.
(15) Manna, L.; Milliron, D. J.; Meisel, A.; Alivisatos. A. P. *Nat. Mater*. **2003**, *2*, 382−385.
(16) Briskman, R. N. *Sol. Energy Mater. Sol. Cells* **1992**, *27*, 361−368.
(17) Poizot, P.; Laruelle, S.; Grugeon, S.; Dupont, L.; Taracon, J. M. *Nature* **2000**, *407*, 496−499.
(18) Ramirez-Ortiz, J.; Medina-Valtierra, T. O. J.; Acosta-Ortiz, S. E.; Bosch, P.; de los Reyes, J. A.; Lara, V. H. *Appl. Surf. Sci*. **2001**, *174*, 177−184.
(19) Hara, M.; Kondo, T.; Komoda, M.; Ikeda, S.; Shinohara, K.; Tanaka, A.; Kondo, J. N.; Domen, K. *Chem. Commun*. **1998**, 357−358.
(20) Wang, W. Z.; Wang, G. H.; Wang, X. S.; Zhan, Y. J.; Liu, Y. K.; Zheng, C. L.; *Adv. Mater*. **2002**, *14*, 67−69.
(21) Wang, D. B.; Mo, M. S.; Yu, D. B.; Xu, L. Q.; Li, F. Q.; Qian, Y. T. *Cryst. Growth Des*. **2003**, *3*, 717−720.
(22) Gou, L. F.; Murphy, C. J. *Nano Lett*. **2003**, *3*, 231−234.
(23) Yang, M.; Zhu, J. J. *J. Cryst. Growth* **2003**, *256*, 134−138.
(24) Chang, Y.; Teo, J. J.; Zeng, H. C. *Langmuir* **2005**, *21*, 1074−1079.
(25) Liu, R.; Oba, F.; Bohannan, E. W.; Ernst, F.; Switzer, J. A. *Chem. Mater*. **2003**, *15*, 4882−4885.
(26) He, P.; Shen, X. H.; Gao, H. C. *J. Colloid. Interface Sci*. **2005**, *284*, 510−515.
(27) Lu, C. H.; Qi, L. M.; Yang, J. H.; Wang, X. Y.; Zhang, D. Y.; Xie, J. L.; Ma, J. L. *Adv. Mater*. **2005**, *17*, 2562−2567.
(28) Murphy, C. J. *Science* **2002**, *298*, 2139−2140.
(29) Wang, Z. L. *J. Phys. Chem. B* **2000**, *104*, 1153−1175.
(30) Lu, C. H.; Qi, L. M.; Yang, J. H.; Zhang, D. Y.; Wu, N. Z.; Ma, J. M. *J. Phys. Chem. B* **2004**, *108*, 17825−17831.